applied sciences

MDPI

Article

Energy-to-Mass Ratio—A Novel Selection Criterion of Pneumatic Motors Used for the Actuation of Wearable Assistive Devices

Andrea Deaconescu and Tudor Deaconescu *

Department of Industrial Engineering and Management, Transilvania University of Brasov, 500036 Brasov, Romania; deacon@unitbv.ro

* Correspondence: tdeacon@unitbv.ro; Tel.: +40-74-575-7850

Abstract: The requirements to be met by a wearable assistive device are compactness, lightweight and energy efficiency. While the literature discusses the construction and performance of such devices, no information is provided as to the criteria to be applied in selecting such an actuator, capable of satisfying the mentioned conditions. Ensuring the high autonomy of a wearable assistive device requires actuators that can store a large quantity of energy in a small as possible volume, for example, actuators with a high energy density. This paper presents a comparative study of the performance of two types of pneumatic actuators: single-acting cylinders and pneumatic muscles, respectively, and offers information that will enable users to select an optimum solution. The quality indicators considered in conducting the comparative study are size, mass, the developed force and the energy-to-mass ratio. A method is proposed to determine the energy developed by the motors over the entire stroke; based on that, the energy-to-mass ratio is subsequently calculated. This indicator is a valuable tool made available to designers of wearable assistive devices. The conclusion yielded by the study asserts that while pneumatic muscles have larger radial and axial dimensions, they present benefits as to the developed forces and the energy-to-mass ratios.

Keywords: pneumatic muscle; single-acting cylinder; wearable assistive device; energy-to-mass ratio

Citation: Deaconescu, A.; Deaconescu, T. Energy-to-Mass Ratio—A Novel Selection Criterion of Pneumatic Motors Used for the Actuation of Wearable Assistive Devices. *Appl. Sci.* **2022**, *12*, 6459. https://doi.org/10.3390/app12136459

Academic Editors: Ionuţ Daniel Geonea and Cristian Copilusi Petre

Received: 8 June 2022
Accepted: 22 June 2022
Published: 25 June 2022

1. Introduction

Mobile robots are capable of moving in a predefined environment and can be autonomous (AMR—autonomous mobile robots) or nonautonomous. The latter deploy guiding devices allowing movement along a predefined navigation route. A significant characteristic of mobile robots is that their moving structure includes all the components that are required for achieving the proposed task, from the energy source to the effectors.

Due to its operational independence mobile robotics lends themselves to a practically unlimited number of applications. In addition to utilization in industry, agriculture or road traffic safety (self-driving motor vehicles), mobile robots can also perform tasks that are potentially dangerous to humans (e.g., disaster control or military applications). Frequently, mobile robots can be found in everyday household applications, such as, for example, semi-autonomous vacuum cleaners [1]. Rehabilitation medicine is another growing field of applicability, where mobile robotics is present in the form of wearable assistive devices.

Wearable assistive devices are designed to facilitate the performance of tasks by persons who, for various reasons, have lost certain abilities. Such devices can be of passive type (not powered) or can be powered by electrical, pneumatic or hydraulic actuation systems.

Orthotic and prosthetic devices fall into the passive category and are externally applied wearable devices: the former being used to modify the structural and functional characteristics of the neuromuscular and skeletal system, while the second is used to replace wholly, or in part, an absent or deficient limb segment [1]. According to the International Society for Prosthetics and Orthotics (ISPO), a prosthetic or orthotic device allows a person with motor

deficiencies to remain active and independent, and to live a normal life without the need for formal support services [2]. Orthotic and prosthetic devices are complex technical systems that, depending on the patient's needs, can be custom-made to exact measurements.

Powered exoskeletons are portable devices of higher complexity. They were developed as augmentative devices to improve the bearer's physical performance or as orthotic devices for the rehabilitation of walking or locomotory assistance. Compared to stationary systems, powered exoskeletons must be compact, lightweight, safe, reliable, intelligent and portable, and can be potentially used at home [3,4].

The mechanical power needed for an exoskeleton is obtained by pneumatic, hydraulic, and electrical actuators. Pneumatic and hydraulic actuation systems, while benefitting from a good power-to-weight ratio, are unattractive from the viewpoint of positioning precision. Electric motors, on the other hand, can be controlled with high precision, while having an unfavorable power-to-weight ratio [5,6]. In [7], Asbeck et al. compare two wearable assistive devices with different actuation systems, pneumatic and electro-mechanical, respectively. The masses of the two systems are 7.1 kg for the pneumatic and 10.1 kg for the electro-mechanical one. The conclusion reached by this study was to choose the pneumatic actuation for wearable assistive suits.

Actuator positioning poses a challenge to designers of powered exoskeletons. Placing the motors near the joints entails a simpler construction, but inertial forces are generated that render the entire system more difficult to control. If the actuators are placed at a distance from the joints, the weight of the mobile components is reduced, but power transmission mechanisms are required that complicate the mechanical structure of the entire assembly.

The growing use of compressed air in the construction of powered exoskeletons is determined by its benefits, such as easy generation and storage, non-flammability, minimum risk of explosion, minimal maintenance requirements of the pneumatic systems, compliance, etc. By their generated motion, pneumatic motors are linear or rotary, and, as to their construction, they are equipped with a piston, blades or membrane [8]. The literature reveals the predominant deployment of pneumatic cylinders and pneumatic muscles in the construction of powered exoskeletons. The main applications of such systems are the rehabilitation and exercising of the upper and lower limbs.

Bae et al. present in [9] the construction of an exoskeleton device for active wrist rehabilitation based on pneumatic cylinders. The flexion and extension of the wrist is conducted by means of a bar system actuated by a pneumatic cylinder. In [10], Goergen et al. put forward a simple and low-cost pneumatic robotic mechanism for lower limb rehabilitation. Operational safety and force control are achieved by adequately adjusting the pressures in the chambers of the pneumatic cylinders that drive the rehabilitation robot. Other exoskeleton devices actuated by pneumatic cylinders are described in papers [11–14].

The utilization of pneumatic muscles is gaining terrain in the construction of wearable assistive devices. This is due to the advantages offered by pneumatic muscles, such as higher force-to-weight ratio and the capacity to generate larger forces than other pneumatic motors. The low weight and flexibility of pneumatic muscles renders them easily integrated into an exoskeleton device [15]. In [16], Bogue presents an overview of recent developments in exoskeletons and robotic prosthetics that highlights the growing presence of pneumatic muscles in this field.

Portable medical systems actuated by pneumatic muscles devised for the rehabilitation of the upper and lower limb joints are presented in a number of publications. Balasubramanian et al. propose in [17] a wearable upper extremity therapy robot, actuated by pneumatic muscles. Abe et al. also use pneumatic muscles to build a soft power support suit for the upper limb [18]. Other examples of deploying pneumatic muscles for the actuation of exoskeletons designed for mobilizing upper and lower limb joints are discussed in papers [19–24]. In [25,26], the authors present two patented applications of pneumatic muscles in the field of medical rehabilitation equipment, designed for the wrist, and hip and knee and ankle, respectively.

In addition to characteristics such as compactness, low mass and portability, the published studies revealed a further significant requirement to be met by a powered exoskeleton, namely the highest possible energy efficiency. While all analyzed papers available in the literature describe the construction and performance of powered exoskeletons, the criteria for selecting a certain type of pneumatic motor (pneumatic cylinder or pneumatic muscle) are not explained.

As a novelty, this paper introduces an energy-related approach to selecting a certain pneumatic actuator. In consideration of the global concern related to energy consumption, the paper presents a method for determining the energy-to-mass ratio (gravimetric energy density) of pneumatic actuators and puts forward this indicator to be used for their selection. Gravimetric energy density is the amount of energy stored in a given system or region of space per unit mass. The higher the gravimetric energy density of the air, the more energy can be stored or transported for the same amount of mass [27].

The reviewed literature discusses this energy-related indicator as a criterion for selecting pneumatic motors only to a rather slight extent. Only in [28], Plettenburg proposes the energy-to-mass ratio as a criterion for selecting a certain type of pneumatic actuator, his calculations yielding the conclusion that the highly praised advantages of pneumatic muscles are exaggerated. Other papers refer to the concept of power-to-weight ratio, without, however, offering a corresponding calculation course [29–31]. Paper [32] presents a comparison of a hydraulic and an electric motor as to their energy efficiency, based on the power-to-mass ratio. The conclusion asserts a higher power density of hydraulic motors compared to that of electric motors.

From all analyzed articles, it followed that regardless of the field of applicability, a certain type of pneumatic actuator is selected generally strictly on economic or technical grounds (dimensions, masses, efficiency, stroke, work pressures, etc.). Starting from these considerations, the paper proposes a methodology for computing the energy-to-mass ratio for two types of pneumatic motors (pneumatic cylinders and muscles, respectively). The presented methodology is new and can be applied to other categories of actuators as well. The comparative study conducted by the authors is also significant for analyzing the possibility of using either type of pneumatic actuator in the construction of powered exoskeletons. It is known that high energy density systems store a larger quantity of energy that in, its turn, ensures the increased autonomy of the rehabilitation system.

For practical purposes pneumatic muscles and pneumatic cylinders of the same manufacturer were selected for the comparative study. Actuators made by other manufacturers have a behavior (performance) similar to those of the studied motors, slight differences existing only in relation to the exterior design.

The aim of the study was to provide the necessary information for a correct selection based on quantifiable quality indicators of the optimum type of pneumatic actuator. The quality indicators considered in the comparative study are size, mass, developed force and the energy-to-mass ratio, meaning the specific energy or gravimetric energy density of an actuator. All of these quantities are easily measured or calculated, thus yielding reliable results.

The main contributions of this paper consist in (i) introducing a computational method of the energy developed by the studied pneumatic actuators and (ii) conducting an energy-to-mass ratio based comparative study of the performance of pneumatic cylinders and pneumatic muscles, respectively.

The paper continues with a second section that describes the studied pneumatic actuators. In the third section, the energy-to-mass ratio is defined, and its values determined for the studied motors. The third section of the paper concludes with two concrete examples of rehabilitation equipment for which the energy-to-mass ratios are calculated. The paper is completed by the conclusions and recommendations resulting from the study. Depending on the comparison criteria that are of interest to a particular user, one or the other variant of pneumatic actuator can be selected.

2. Pneumatic Muscles vs. Pneumatic Cylinders

The proposed working method consists of going through a number of steps with the aim of obtaining the energy-to-mass ratio. The sequence of steps is as follows:

- Computation of the forces developed by the analyzed pneumatic actuators;
- Determining the required dimensional specifications of the analyzed actuators;
- Establishing the dependency of the actuators mass on the length of the stoke;
- Determining the dependency equations of the forces developed by the actuators versus stroke.

Based on these data, subsequently, the energy-to-mass ratio is calculated.

2.1. Computation of the Forces Developed by the Analyzed Pneumatic Actuators

A number of papers on applications of pneumatic muscle assert that this type of actuator offers more advantages than pneumatic cylinders, without, however, following up with concrete arguments in this respect. Some of the advantages of pneumatic muscles enumerated in [33] are:

- The developed initial force is significantly larger at the same diameter;
- Small mass per unit force;
- Smaller consumption of compressed air;
- Superior energy density, etc.

In order to prove these assertions, further discussion on the authors present and a comparison between single-acting pneumatic cylinders and pneumatic muscles manufactured by Festo are presented (Figure 1). These specific actuators were selected for the study because the forces developed by them have similar evolutions over the length of the stroke. The maximum force is developed at the beginning and reaches its minimum by the end of the stroke.

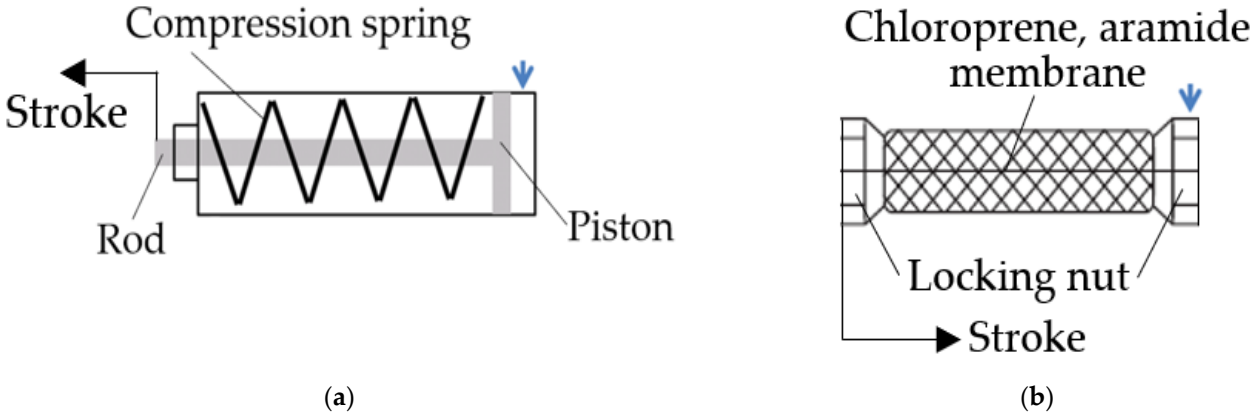

Figure 1. Types of studied pneumatic motors: (**a**) Single-acting cylinder; (**b**) Pneumatic muscle.

In the case of single-acting cylinders, compressed air is applied to a single face of the piston and, consequently, motion is generated in a single direction. The piston is then reversed automatically by means of a built-in spring. The force developed by a cylinder of this type is calculated by Equation (1):

$$F = p \times \frac{\pi \cdot D^2}{4} - F_{FR} - F_{Spr} \quad (1)$$

where p is the pressure of the compressed air, D—the piston diameter, F_{FR}—the friction forces, F_{Spr}—the spring force.

The pneumatic muscle generates displacement by changing its geometrical form when fed compressed air. As the air pressure increases, a traction force acting along the muscle axis causes it to shorten. Such axial contraction represents the stroke of the motor. The maximum axial contraction is of about 20% of the muscle's initial length. The axial

force is maximum at the onset of contraction and falls to zero as the end of the stroke is reached. The force developed by a pneumatic muscle is calculated by Equation (2) [30]:

$$F = p \times \frac{\pi}{4} \times d^2 \times \left[\frac{3 \times \cos^2 \alpha - 1}{1 - \cos^2 \alpha}\right] \quad (2)$$

where p is the working pressure, d the diameter of the pneumatic muscle, and α is the winding angle of the synthetic fiber tissue the envelopes the inner tube of the muscle.

The following models of the two types of pneumatic motors were selected for the purpose of this comparative study:

- Round cylinders, single-acting, pushing, based on ISO 6432, manufactured by FESTO, Esslingen, Germany, shown in Figure 2a [34];
- Pneumatic muscles, models DMSP-xx-N, manufactured by FESTO, Esslingen, Germany, shown in Figure 2b [35].

(**a**) (**b**)

Figure 2. Studied pneumatic motors: (**a**) Single-acting cylinder (ESNU) [34]; (**b**) Pneumatic muscle (DMSP) [35].

2.2. Determining the Required Dimensional Specifications of the Analyzed Actuators

Three sizes of each motor type were selected and paired for comparison. For each pair of compared motors, the active diameters and the strokes were the same. Table 1 presents the characteristics of these pneumatic motors [34,35]:

Table 1. Characteristics of the studied pneumatic motors.

Motor Type	Motor Code	Interior Diameter [mm]	Stroke Length [mm]
Round cylinders	ESNU-10-50-P-A	10	50
	ESNU-20-50-P-A	20	50
	ESNU-40-50-P-A	40	50
Pneumatic muscles	DMSP-10-250N-RM-CM	10	50
	DMSP-20-250N- RM-CM	20	50
	DMSP-40-250N- RM-CM	40	50

A comparison of the two types of pneumatic motors used for the evaluation criteria their dimensions, masses, developed forces and the energy-to-force ratio.

From the viewpoint of sizes, Table 2 features the main dimensions of the two types of motors, as indicated in their technical specifications [34,35].

Notably, single-acting cylinders are of smaller axial and radial dimensions, which may represent an advantage for building compact powered exoskeletons.

Table 2. Dimensions of the studied pneumatic motors.

Motor Type	Motor Code	Maximum Exterior Diameter [mm]	Total Stroke Length [mm]
Round cylinders	ESNU-10-50-P-A	16	86
	ESNU-20-50-P-A	30	132
	ESNU-40-50-P-A	50	177.6
Pneumatic muscles	DMSP-10-250N-RM-CM	30.1	318.2
	DMSP-20-250N-RM-CM	45.6	335
	DMSP-40-250N-RM-CM	65.5	361

2.3. Establishing the Dependency of the Actuators Mass on the Length of the Stoke

The masses of the pneumatic motors depend on the lengths of their strokes and their axial and radial dimensions. In the case of single-acting cylinders based on their technical specifications, the equations of mass versus stroke variations can be determined:

$$m_{\text{ESNU\_10}}(s) = 0.27 \times s + 0.0373 \quad (3)$$

$$m_{\text{ESNU\_20}}(s) = 0.72 \times s + 0.1868 \quad (4)$$

$$m_{\text{ESNU\_40}}(s) = 2.4 \times s + 0.661 \quad (5)$$

In the three equations, the masses m are calculated in kg and the stroke length s is entered in meters.

Equations (6)–(8) describe the variation in the mass of a pneumatic muscle (in kg) versus the length l (in meters) of its active part (excluding the end connections). The equations resulted from the information included in the technical specifications of the pneumatic muscles.

$$m_{\text{DMSP\_10}}(l) = 0.094 \times l + 0.077 \quad (6)$$

$$m_{\text{DMSP\_20}}(l) = 0.178 \times l + 0.238 \quad (7)$$

$$m_{\text{DMSP\_40}}(l) = 0.34 \times l + 0.675 \quad (8)$$

It is known that upon being fed compressed air, the pneumatic muscle contracts by up to 20% of its initial length. The maximum stroke carried out by the free end of the muscle is described by Equation (9):

$$s = \Delta l = 0.2 \times l \quad (9)$$

Thus, the equations describing the variation in the mass of the pneumatic muscles versus the stroke s becomes:

$$m_{\text{DMSP\_10}}(s) = 0.47 \times s + 0.077 \quad (10)$$

$$m_{\text{DMSP\_20}}(s) = 0.89 \times s + 0.238 \quad (11)$$

$$m_{\text{DMSP\_40}}(s) = 1.7 \times s + 0.675 \quad (12)$$

Table 3 includes the masses of the six studied pneumatic motors, and Figure 3 shows the variation lines of the masses of the two types of motors versus their strokes.

Table 3. Masses of the studied pneumatic motors.

Motor Dimension [mm]	Mass Calculated for a 50 mm Stroke [kg]	
	ESNU	DMSP
10	0.0508	0.1005
20	0.2228	0.2825
40	0.795	0.76

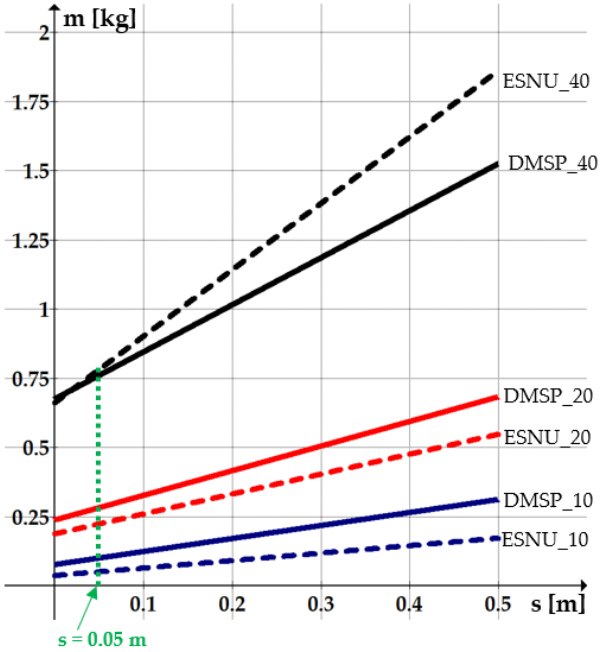

Figure 3. Dependency of the masses of the studied pneumatic motors on the stroke (m = f(s)).

The values in Table 3 and the lines in Figure 3 suggest that for the same diameter of the motors, their masses do not differ significantly. For diameters of 10 mm and 20 mm, single-acting cylinders have a slightly smaller mass, while at 40 mm diameter it is the pneumatic muscle that has the smaller mass. In the case of 40 mm diameter actuators, both cylinders and muscles, as the strokes required to be carried out and implicitly their lengths increase, the difference between cylinder and muscle mass increases, i.e., the pneumatic muscles become increasingly lighter than the cylinders.

2.4. Determining the Dependency Equations of the Forces Developed by the Actuators Versus Stroke

Tables 4 and 5 feature the variability intervals of the forces developed by the six pneumatic motors. All presented values were determined for a maximum pressure of 6 bar, and the data were taken from the technical specifications of the pneumatic motors.

Table 4. Forces developed by the ESNU pneumatic cylinders.

Motor Code	Maximum Force [N]	Minimum Force [N]
ESNU-10-50-P-A	41	4.8
ESNU-20-50-P-A	169	13.6
ESNU-40-50-P-A	688	30

Table 5. Forces developed by the DMSP pneumatic muscles.

Motor Code	Specific Axial Contraction ε = s/l					
	0	0.04	0.08	0.12	0.16	0.20
	Stroke [m]					
	0	0.01	0.02	0.03	0.04	0.05
	Developed Force [N]					
DMSP-10-250N- RM-CM	397.4	318.8	226.6	154.4	90.9	32.1
DMSP-20-250N- RM-CM	1199.1	1175.5	910.8	691.5	498.1	310
DMSP-40-250N- RM-CM	3994.7	3852.3	3712.3	2852.3	2126.3	1489.6

Based on the data in Tables 4 and 5, the lines and curves shown in Figures 4 and 5 were plotted that describe the dependency of the forces developed by the pneumatic motors on the stroke. The dependencies are expressed by Equations (13)–(18).

$$F_{\text{ESNU\_10}}(s) = -724 \times \text{s} + 41 \quad (13)$$

$$F_{\text{ESNU\_20}}(s) = -3108 \times \text{s} + 169 \quad (14)$$

$$F_{\text{ESNU\_40}}(s) = -97656 \times \text{s} + 6372.4 \quad (15)$$

$$F_{\text{DMSP\_10}}(s) = 5.3333 \times 10^5 \times s^3 - 1821.4286 \times s^2 - 8556.5476 \times s + 398.95 \quad (16)$$

$$F_{\text{DMSP\_20}}(s) = 1.0866 \times 10^7 \times s^3 - 9.1088 \times 10^5 \times s^2 + 549.1005 \times s + 1211.2778 \quad (17)$$

$$F_{\text{DMSP\_40}}(s) = 2.7745 \times 10^7 \times s^3 - 2.9408 \times 10^6 \times s^2 + 2.7968 \times 10^4 \times s + 3960.6746 \quad (18)$$

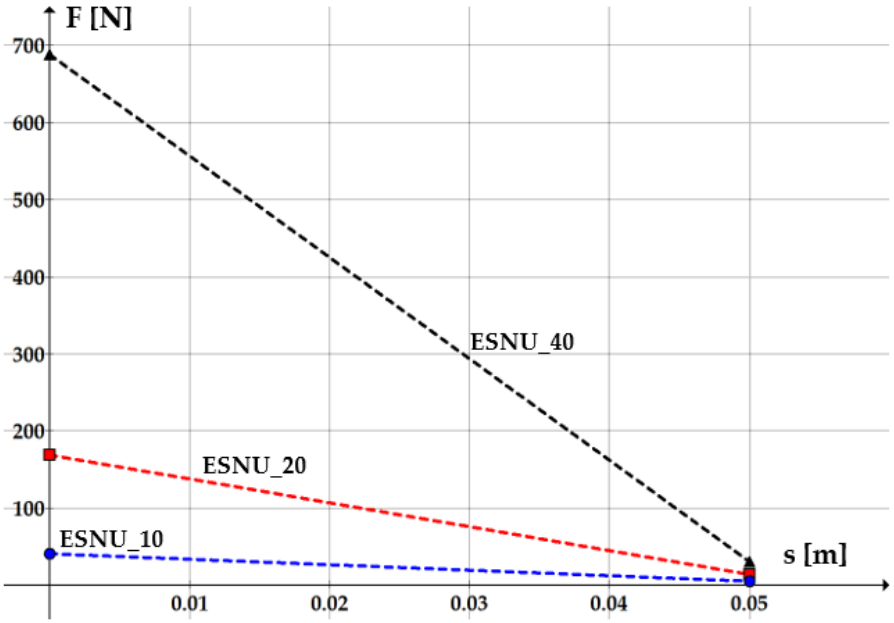

Figure 4. Variation of the forces developed by the studied pneumatic cylinders.

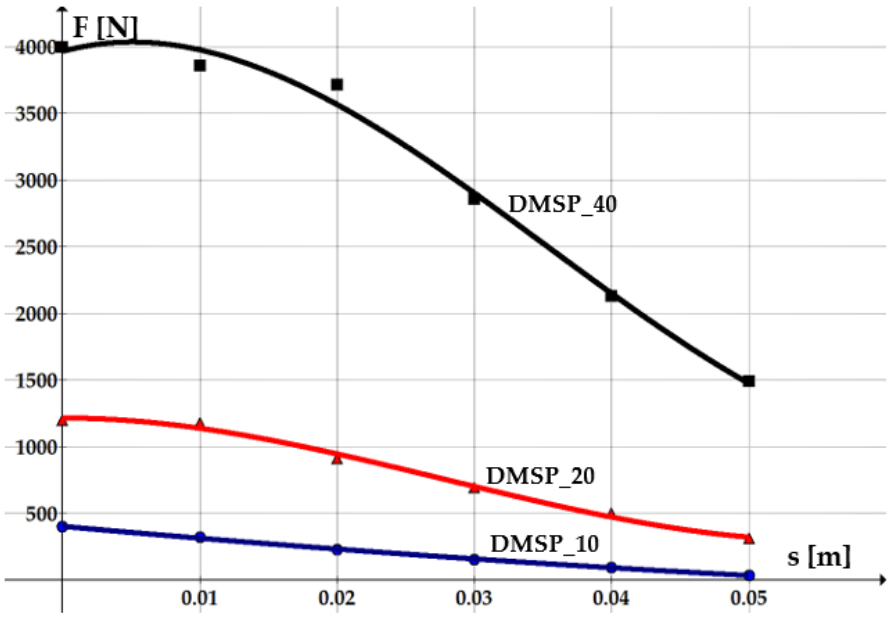

Figure 5. Variation of the forces developed by the studied pneumatic muscles.

Figures 4 and 5 show that the forces developed by pneumatic muscles are about 5 to 10 times greater than those developed by single-acting cylinders.

3. Determination of the Energy-to-Mass Ratio

The energy-to-mass ($R_{E/m}$) ratio is a quantity devised for comparing the energy efficiency of different types of actuators. In [26], Plettenburg proposes the computational relationship of this indicator:

$$R_{\frac{E}{m}} = \frac{\int F(s)\cdot ds}{m(s)} \tag{19}$$

where $F(s)$ is the force developed by the pneumatic motor, s is the stroke and m is the mass of the motor.

For pneumatic muscles, Equation (19) is adapted by taking into account the specific axial contraction $\varepsilon = s/l$:

$$R_{\frac{E}{m}} = \frac{l\cdot \int F(\varepsilon)\cdot d\varepsilon}{m(s)} = \frac{\int F(s)\cdot ds}{m(s)} \tag{20}$$

The numerator in Equations (19) and (20) represents the energy developed by the motors over the entire stroke and is obtained by the integration of the force Equations (13)–(18). The integrals in the numerator represent the surfaces between the variation curves of the forces, the abscissa of the graphs and the maximum and minimum limits of the motors' displacements. Figure 6 highlights these surfaces for the ESNU cylinders and the DMSP pneumatic muscles.

Equations (21)–(23) represent the calculation formulae of the energy-to-mass ratios for the three studied pneumatic cylinders:

$$R_{\frac{E}{m},\,\mathrm{ESNU\_10}} = \frac{1.145}{0.27 \times \mathrm{s} + 0.0373} \tag{21}$$

$$R_{\frac{E}{m},\,\mathrm{ESNU\_20}} = \frac{4.565}{0.72 \times \mathrm{s} + 0.1868} \tag{22}$$

$$R_{\frac{E}{m},\,\mathrm{ESNU\_40}} = \frac{17.95}{2.4 \times \mathrm{s} + 0.661} \tag{23}$$

For the pneumatic muscles, first the equations of the energies developed over the working interval are determined. Figure 6b shows the surface that materializes the integrals in Equation (20).

$$E_{\mathrm{DMSP\_10}}(s) = \int_0^{0.05} F_{\mathrm{DMSP\_10}}(s)\cdot ds = 10.0093 \tag{24}$$

$$E_{\mathrm{DMSP\_20}}(s) = \int_0^{0.05} F_{\mathrm{DMSP\_20}}(s)\cdot ds = 40.2748 \tag{25}$$

$$E_{\mathrm{DMSP\_40}}(s) = \int_0^{0.05} F_{\mathrm{DMSP\_40}}(s)\cdot ds = 153.8121 \tag{26}$$

The energy-to-mass ratios of the three pneumatic muscles will be:

$$R_{\frac{E}{m},\,\mathrm{DMSP\_10}} = \frac{E_{\mathrm{DMSP\_10}}(s)}{m_{\mathrm{DMSP\_10}}(s)} = \frac{10.0093}{0.47 \times s + 0.077} \tag{27}$$

$$R_{\frac{E}{m},\mathrm{DMSP\_20}} = \frac{E_{\mathrm{DMSP\_20}}(s)}{m_{\mathrm{DMSP\_20}}(s)} = \frac{40.2748}{0.89 \times s + 0.238} \tag{28}$$

$$R_{\frac{E}{m},\,\mathrm{DMSP\_40}} = \frac{E_{\mathrm{DMSP\_40}}(s)}{m_{\mathrm{DMSP\_40}}(s)} = \frac{153.8121}{1.7 \times s + 0.675} \tag{29}$$

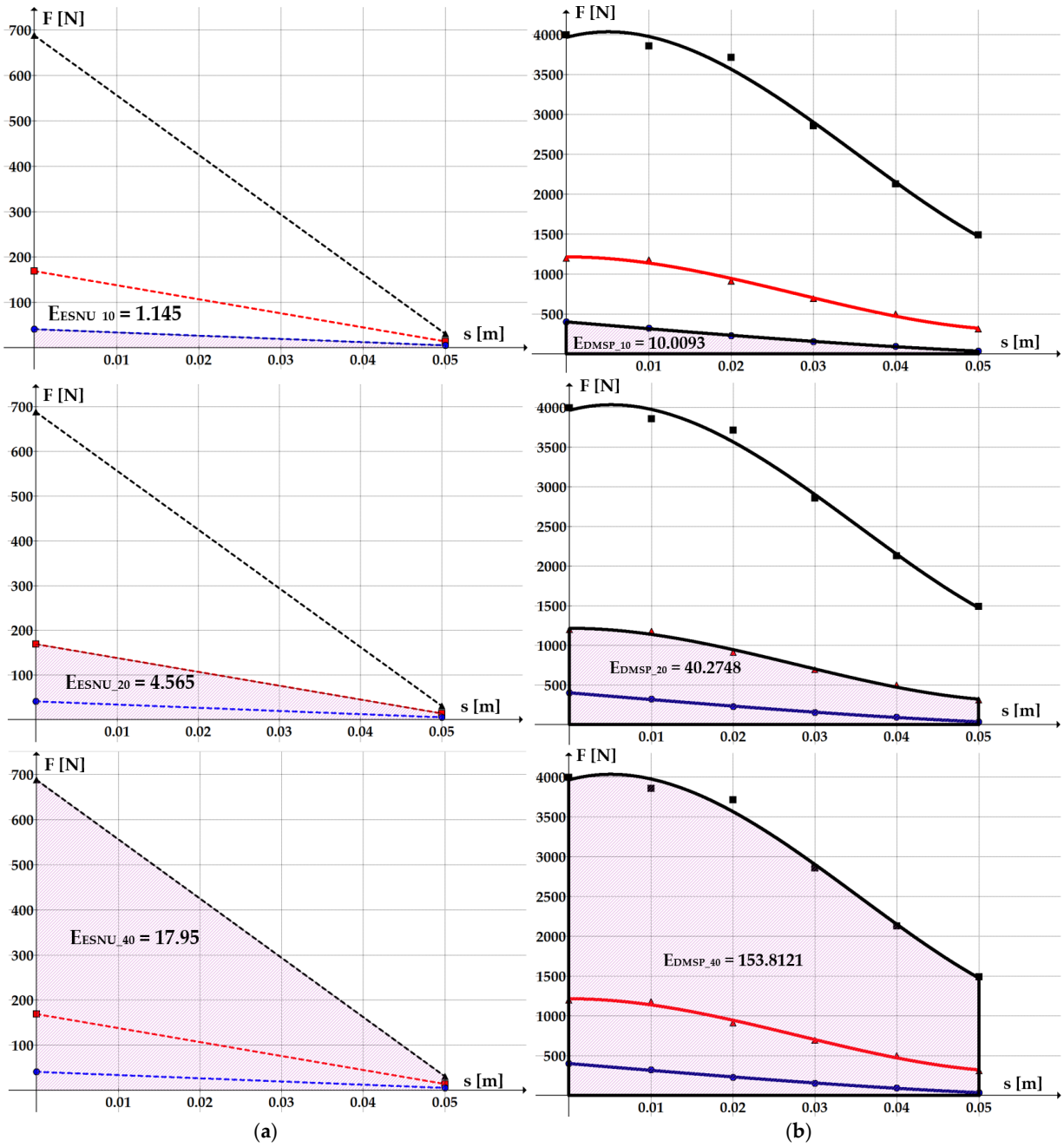

Figure 6. Energy developed by: (**a**) ESNU pneumatic cylinders; (**b**) DMSP pneumatic muscles.

Figure 7 shows the variation in the energy-to-mass ratios versus stroke for the six pneumatic motors and Table 6 presents the values of these ratios for a 50 mm stroke.

Table 6. Energy-to-mass ratios of the studied pneumatic motors.

Motor Dimension [mm]	Energy-to-Mass Ratio for a 50 mm Stroke [Nm/kg]	
	ESNU	**DMSP**
10	22.5394	99.595
20	20.4892	142.5657
40	22.9834	202.3843

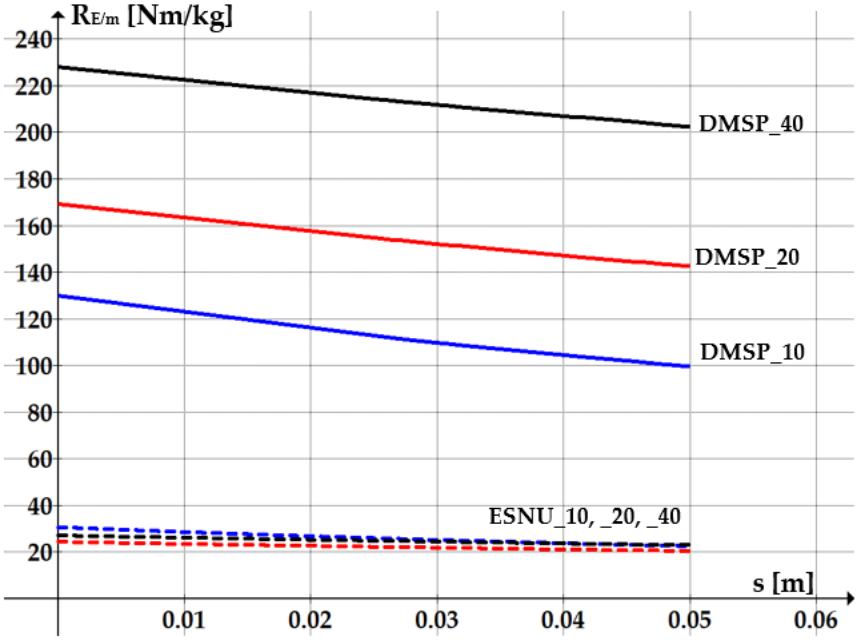

Figure 7. Variation of the energy-to-mass ratios versus strokes of the pneumatic motors.

Figure 7 reveals that in the case of single-acting cylinders, the values of the energy-to-mass ratios are approximately the same regardless of their diameters. This observation does not apply in the case of pneumatic muscles, where the energy-to-mass ratio in a 40 mm diameter muscle is about two-times larger than that in a 10 mm diameter one.

The above table shows that for the studied pneumatic actuators with a 50 mm stroke, the energy-to-mass ratios of the pneumatic muscles are about 4- to 9-times larger than those of single-acting cylinders. Consequently, from the viewpoint of energy efficiency, pneumatic muscles are recommended for applications that require the development of a large force while ensuring maximum energy efficiency.

Table 7 presents an overview of the results obtained by the comparative study of the two types of linear pneumatic motors. The (+) sign indicates a favorable characteristic while (−) indicates a disadvantage.

Table 7. Overview of the results obtained by the comparative study of the two types of pneumatic motors.

Motor Type	Maximum Exterior Diameter	Total Length	Mass	Force	Energy-to-Mass Ratio
Round cylinders ESNU	+	+	=	−	−
Pneumatic muscles DMSP	−	−	=	+	+

In articles [25,26], the authors have presented and discussed two pieces of medical rehabilitation equipment, one designed for the recovery of the lower limb (Figure 8), and the other for the recovery of the wrist (Figure 9). Both devices are actuated by pneumatic muscles, a technical solution selected due to the favorable energy-to-mass ratio.

For these devices, Table 8 features a comparison of the computational results obtained by the method proposed in this paper. The values of the energy-to-mass ratios of the utilized pneumatic muscles were compared to those of the single-acting cylinders that could have been used alternatively as actuators of the two devices. Table 8 includes the dimensions of the compared actuators.

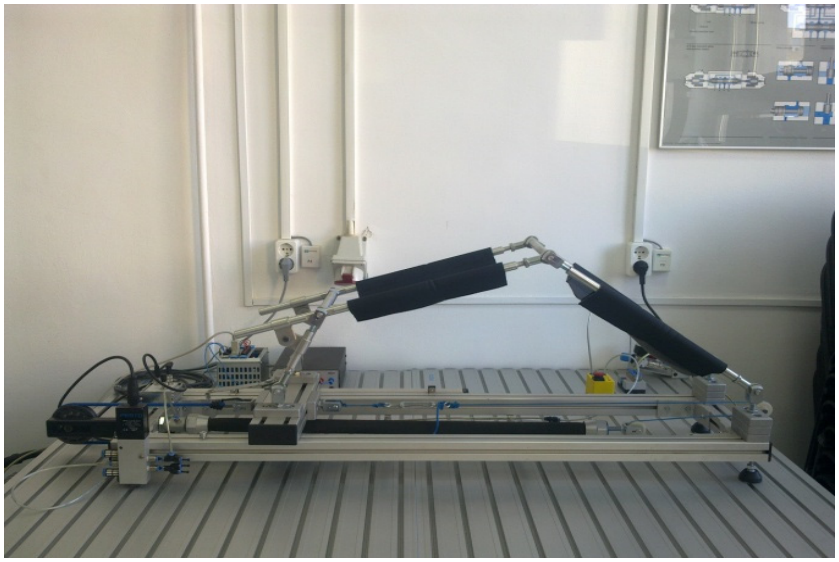

Figure 8. Assistive rehabilitation device for the joints of the lower limb.

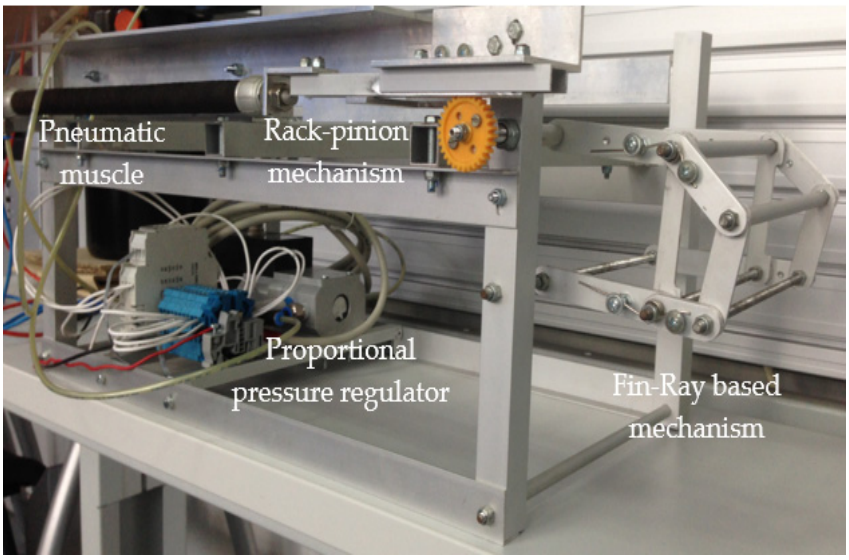

Figure 9. Pneumatic muscle actuated wrist rehabilitation equipment.

Table 8. Comparison of the energy-to-mass ratios computed for the two types of actuators.

	Energy-to-Mass Ratio [Nm/kg]
Assistive rehabilitation device for the joints of the lower limb	
Pneumatic muscle L = 750 mm; d = 20 mm; s = 150 mm	108.4113
Single-acting cylinder D = 20 mm; s = 150 mm	15.4851
Wrist rehabilitation equipment	
Pneumatic muscle L = 300 mm; d = 10 mm; s = 60 mm	95.1454
Single-acting cylinder D = 10 mm; s = 60 mm	21.4019

It needs be pointed out that in the case of the assistive rehabilitation device for the joints of the lower limb, the value of the energy-to-mass ratio a of the pneumatic muscle is

7-times greater than that of the equivalent single-acting cylinder, while in the case of the wrist rehabilitation equipment, the proportion is of 4.45. These two examples confirm the superior behavior of pneumatic muscles from the energy point of view.

4. Conclusions

Thus, the methodology for determining the energy-to-mass ratio entails a sequence of steps consisting of (i) computing the actuator's mass; (ii) determining the evolution of the force developed over the entire working stroke; (iii) computing the developed energy and (iv) computing the energy-to-mass ratio. Given its short running time, the computational methodology of the energy-to-mass ratio put forward in the paper also lends itself to other types of actuators.

The following conclusions resulted in relation to the quality characteristics used and analyzed for the comparison of the two types of pneumatic actuators:

- From the viewpoint of axial and radial dimensions, single-acting cylinders are more compact than pneumatic muscles;
- The masses of the two types of pneumatic motors of the same diameter do not differ significantly. Nevertheless, in the case of 40 mm diameter actuators, as the strokes required to be carried out and implicitly their lengths increase, the difference between the mass of the cylinder and that of the muscle increases, in the sense that the pneumatic muscles become increasingly lighter than the cylinders.
- The forces developed by pneumatic muscles are about 5- to 10-times greater than those developed by single-acting cylinders;
- The energy-to-mass ratios of the pneumatic muscles are about 4- to 9-times larger than those of single-acting cylinders.

The results of the study prove that despite their radial and axial larger sizes, pneumatic muscles offer benefits from the viewpoint of developed forces and energy-to-mass ratios. In applications that require large forces and high energy efficiency, replacing single-acting cylinders with pneumatic muscles has become a necessity.

The analysis of the energy-to-mass ratios confirm the assertions found in the literature related to pneumatic muscles that motors have an energy efficiency superior to that of single-acting pneumatic cylinders.

The flexibility of pneumatic muscles, the large, developed forces and a high energy-to-mass ratio render these actuators an optimum solution for manufacturing exoskeleton devices. In addition, their light weight, portability, safe operation, reliability, compliance and easy integration in wearable assistive devices render pneumatic muscles a viable actuation alternative to such rehabilitation systems.

Author Contributions: Conceptualization, A.D. and T.D.; methodology, A.D. and T.D.; resources, A.D.; data curation, T.D.; writing—original draft preparation, A.D.; writing—review and editing, A.D. and T.D.; supervision, A.D. All authors have read and agreed to the published version of the manuscript.

Funding: This research received no external funding.

Institutional Review Board Statement: Not applicable.

Informed Consent Statement: Not applicable.

Data Availability Statement: Not applicable.

Conflicts of Interest: The authors declare no conflict of interest.

References

1. Harmonic Drive SE. Mobile Robotics. Available online: https://harmonicdrive.de/en/glossary/mobile-robotics (accessed on 17 January 2022).
2. International Society for Prosthetics and Orthotics. Prosthetics and orthotics services. Available online: https://www.ispoint.org/page/POservices (accessed on 18 January 2022).

3. Sirlantzis, K.; Larsen, L.B.; Kanumuru, L.K.; Oprea, P. Robotics. In *Handbook of Electronic Assistive Technology*; Cowan, D., Najafi, L., Eds.; Elsevier Ltd.: London, UK, 2019; pp. 311–345.
4. Martinez-Hernandez, U.; Metcalfe, B.; Assaf, T.; Jabban, L.; Male, J.; Zhang, D. Wearable Assistive Robotics: A Perspective on Current Challenges and Future Trends. *Sensors* **2021**, *21*, 6751. [CrossRef] [PubMed]
5. Gopura, R.A.R.C.; Bandara, D.S.V.; Kiguchi, K.; Mann, G.K.I. Developments in hardware systems of active upper-limb exoskeleton robots: A review. *Robot. Auton. Syst.* **2016**, *75*, 203–220. [CrossRef]
6. Knaepen, K.; Beyl, P.; Duerinck, S.; Hagman, F.; Lefeber, D.; Meeusen, R. Human-robot interaction: Kinematics and muscle activity inside a powered compliant knee exoskeleton. *IEEE Trans. Neural. Syst. Rehabil. Eng.* **2014**, *22*, 1128–1137. [CrossRef] [PubMed]
7. Asbeck, A.T.; De Rossi, S.M.M.; Galiana, I.; Ding, Y.; Walsh, C.J. Stronger, Smarter, Softer: Next-Generation Wearable Robots. *IEEE Robot. Autom. Mag.* **2014**, *21*, 22–23. [CrossRef]
8. Deaconescu, T.; Deaconescu, A. Linear pneumatic motors—A comparative study. *MATEC Web Conf.* **2017**, *112*, 5007. [CrossRef]
9. Bae, J.; Moon, I. Design and control of an exoskeleton device for active wrist rehabilitation. In Proceedings of the 12th International Conference on Control, Automation and Systems, Jeju, Korea, 17–21 October 2012; pp. 1577–1580.
10. Goergen, R.; Valdiero, A.C.; Rasia, L.A.; Oberdörfer, M.; de Souza, J.P.; Gonçalves, R.S. Development of a Pneumatic Exoskeleton Robot for Lower Limb Rehabilitation. In Proceedings of the IEEE 16th International Conference on Rehabilitation Robotics (ICORR), Toronto, ON, Canada, 24–28 June 2019; pp. 187–192.
11. Pavithrana, A.; Skariaa, E.; Rajana, R.; Joseb, J. Design and fabrication of a Pneumatic Exoskeleton. *Int. J. of Adv. Res. Trends Eng. Technol.* **2017**, *4*, 36–42.
12. Krishna, G.; Hosmutt, P.; Nyamagoud, B.M.; Patil, M.V.; Hunnur, O. Design and Fabrication of Pneumatic Powered Exoskeleton Suit for Arms. *Int. Res. J. Eng. Tech.* **2018**, *5*, 4415–4419.
13. Henderson, G.C. Pneumatically-Powered Robotic Exoskeleton to Exercise Specific Lower Extremity Muscle Groups in Humans. Master's Thesis, Georgia Institute of Technology, Atlanta, GA, USA, 20 March 2012.
14. Pavana, K.B.; Krisantha, A.P.; Pereira, R.M.; Sahil, M.A.; Varun, S.; Mallya, V.S. Design and Fabrication of a Pneumatically Powered Human Exoskeleton Arm. *J. Mech. Eng. Autom.* **2017**, *7*, 85–88.
15. Thalman, C.; Artemiadis, P. A review of soft wearable robots that provide active assistance: Trends, common actuation methods, fabrication, and applications. *Wearable Technol.* **2020**, *1*, E3. [CrossRef]
16. Bogue, R. Exoskeletons and robotic prosthetics: A review of recent developments. *Ind. Robot.* **2009**, *36*, 421–427. [CrossRef]
17. Balasubramanian, S.; Wei, H.R.; Perez, M.; Shepard, B.; Koeneman, E.; Koeneman, J.; He, J. Rupert: An exoskeleton robot for assisting rehabilitation of arm functions. In Proceedings of the 2008 Virtual Rehabilitatio, Vancouver, BC, Canada, 25–27 August 2008; pp. 163–167.
18. Abe, T.; Koizumi, S.; Nabae, H.; Endo, G.; Suzumori, K.; Sato, N.; Adachi, M.; Takamizawa, F. Fabrication of "18 Weave" muscles and their application to soft power support suit for upper limbs using thin McKibben muscle. *IEEE Robot. Autom. Lett.* **2019**, *4*, 2532–2538. [CrossRef]
19. Andrikopoulos, G.; Nikolakopoulos, G.; Manesis, S. Motion Control of a Novel Robotic Wrist Exoskeleton via Pneumatic Muscle Actuators. In Proceedings of the IEEE 20th Conference on Emerging Technologies & Factory Automation (ETFA), Luxembourg, 8–11 September 2015.
20. Zhang, J.F.; Yang, C.J.; Chen, Y.; Zhang, Y.; Dong, Y.M. Modeling and control of a curved pneumatic muscle actuator for wearable elbow exoskeleton. *Mechatronics* **2008**, *18*, 448–457. [CrossRef]
21. Tsagarakis, N.; Caldwell, D.G.; Medrano-Cerda, G.A. A 7 DOF pneumatic muscle actuator (pMA) powered exoskeleton. In Proceedings of the 8th IEEE International Workshop on Robot and Human Interaction, Pisa, Italy, 27–29 September 1999.
22. Nassour, J.; Zhao, G.; Grimmer, M. Soft pneumatic elbow exoskeleton reduces the muscle activity, metabolic cost and fatigue during holding and carrying of loads. *Sci. Rep.* **2021**, *11*, 12556. [CrossRef] [PubMed]
23. Chen, C.-T.; Lien, W.-Y.; Chen, C.-T.; Wu, Y.-C. Implementation of an Upper-Limb Exoskeleton Robot Driven by Pneumatic Muscle Actuators for Rehabilitation. *Actuators* **2020**, *9*, 106. [CrossRef]
24. Irshaidat, M.; Soufian, M.; Al-Ibadi, A.; Nefti-Meziani, S. A Novel Elbow Pneumatic Muscle Actuator for Exoskeleton Arm in Post-Stroke Rehabilitation. In Proceedings of the 2nd IEEE International Conference on Soft Robotics (RoboSoft), Seoul, Korea, 14–18 April 2019; pp. 630–635.
25. Deaconescu, T.; Deaconescu, A. Pneumatic Muscle Actuated Equipment for Continuous Passive Motion. In *IAENG Transactions on Engineering Technologies*; Ao, S.L., Chan, A.H.S., Katagiri, H., Xu, L., Eds.; Springer: Dordrecht, The Netherlands, 2009; Volume 3, pp. 311–321.
26. Petre, I.; Deaconescu, A.; Sârbu, F.; Deaconescu, T. Pneumatic Muscle Actuated Wrist Rehabilitation Equipment Based on the Fin Ray Principle. *Stroj. Vestn. J. Mech. Eng.* **2018**, *64*, 383–392.
27. Energy Density. Available online: https://en.wikipedia.org/wiki/Energy_density (accessed on 20 June 2022).
28. Plettenburg, D.H. Pneumatic Actuators: A Comparison of Energy-to-Mass Ratio's. In Proceedings of the 2005 IEEE 9th International Conference on Rehabilitation Robotics, Chicago, IL, USA, 28 June–1 July 2005; pp. 545–549.
29. Tsagarakis, N.; Caldwell, D.G. Improved modelling and assessment of pneumatic muscle actuators. In Proceedings of the IEEE International Conference on Robotics & Automation, San Francisco, CA, USA, 24–28 April 2000; pp. 3641–3646.

30. Medrano-Cerda, G.A.; Bowler, C.J.; Caldwell, D.G. Adaptive position control of antagonistic pneumatic muscle actuators. In Proceedings of the IEEE/RSJ International Conference on Intelligent Robots and Systems, Pittsburgh, PA, USA; 1995; pp. 378–383.
31. Nakamura, N.; Sekiguchi, M.; Kawashima, K.; Fujita, T.; Kagawa, T. Developing a robot arm using pneumatic artificial rubber muscles. In Proceedings of the Bath Workshop on Power Transmission & Motion Control, Bath, UK, 15 September 2002; pp. 365–375.
32. Sakama, S.; Tanaka, Y.; Kamimura, A. Characteristics of Hydraulic and Electric Servo Motors. *Actuators* **2022**, *11*, 11. [CrossRef]
33. Hesse, S. *The Fluidic Muscle in Application*; Blue Digest on Automation: Esslingen, Germany, 2003; pp. 27–28.
34. Round Cylinders ESNU. Available online: https://www.festo.com/cat/en-gb_gb/data/doc_ENGB/PDF/EN/ESNU_EN.PDF (accessed on 12 December 2021).
35. Fluidic Muscle DMSP/MAS. Available online: https://www.festo.com/rep/en_corp/assets/pdf/info_501_en.pdf (accessed on 12 December 2021).